



New paleomagnetic data from Oligocene–upper Miocene sediments in the Rif chain (northern Morocco): Insights on the Neogene tectonic evolution of the Gibraltar arc

Francesca Cifelli,¹ Massimo Mattei,¹ and Massimiliano Porreca¹

Received 16 July 2007; revised 26 October 2007; accepted 10 December 2007; published 28 February 2008.

[1] In this paper, we present new paleomagnetic data from Tertiary sedimentary sequences of the Rif chain. Paleomagnetic results show that the Rif chain underwent different patterns of vertical axis rotations depending on the tectonic location of the sampled sites. Whereas no paleomagnetic rotations have been measured either in the upper Miocene postnappe basins located along the Mediterranean coast or in the upper Miocene Fes-Taza foreland basins, upper Miocene thrust top sequences from the external Rif show a significant amount ($20^\circ \pm 13^\circ$ in average) of counterclockwise rotations. The spatial distribution of paleomagnetic rotations shows that tectonic rotations, as observed in other arcs of the Mediterranean region, are confined to the orogenic wedge and do not extend to the foreland domain. Paleomagnetic results from this study contribute to better constrain the age of paleomagnetic rotations in the Rif chain, showing that counterclockwise rotations, previously measured only in Mesozoic units, extended into upper Miocene deposits. These results, together with recent published data from the Betics, suggest that the bending of the Gibraltar Arc was not completely achieved by the late Tortonian–Messinian, enhancing the role of vertical axis rotations in the late Miocene to Recent tectonic evolution of the Gibraltar Arc.

Citation: Cifelli, F., M. Mattei, and M. Porreca (2008), New paleomagnetic data from Oligocene–upper Miocene sediments in the Rif chain (northern Morocco): Insights on the Neogene tectonic evolution of the Gibraltar arc, *J. Geophys. Res.*, *113*, B02104, doi:10.1029/2007JB005271.

1. Introduction

[2] The Rif thrust belt is part of the Alpine orogenic system and, together with the Tell, fringes the Maghrebian Mediterranean coast. These belts are connected to the west with the Betic Cordillera through the Straits of Gibraltar to form the narrow shaped Gibraltar Arc. Different models have been proposed to explain how westward thrusting around the Straits of Gibraltar could have occurred coevally with extension in the Alboran Sea, in the framework of the African-European convergence. The more popular are (1) back-arc extension driven by the westward rollback of an eastward subducting slab [Faccenna *et al.*, 2004; Frizon de Lamotte *et al.*, 1991; Jolivet and Faccenna, 2000; Lonergan and White, 1997; Morales *et al.*, 1999; Royden, 1993]; (2) breakoff of a subducting lithospheric slab [Blanco and Spakman, 1993]; and (3) extensional collapse of an earlier collisional Betic-Rif orogen caused by convective removal of deep lithospheric roots [Platt and Vissers, 1989], slab detachment [Blanco and Spakman, 1993; Zeck, 1999], or delamination of the lithospheric mantle [García-Dueñas *et al.*, 1992; Seber *et al.*, 1996]. Most of these tectonic models are focused on Oligo-

cene-Miocene evolution of the Gibraltar Arc–Alboran Sea region and they assume that the geodynamic processes responsible for the curvature of the Gibraltar Arc and opening of the Alboran Sea were almost complete in late Tortonian. In this scenario, the distribution of present-day deformation and active faulting in the Rif chain reflects a change in the geodynamic regime of this region. Accordingly, the ongoing deformation in the Rif and the Alboran Sea should be mostly controlled by the kinematics of the Eurasia (Iberia)-Nubia plate boundary that is presently located along the northern edge of the African continent [Biggs *et al.*, 2006; Mc Clusky *et al.*, 2003; Meghraoui *et al.*, 1996]. Meghraoui *et al.* [1996] suggest that the late Miocene to Recent deformation in the Rif has been mainly controlled by WNW oriented right-lateral and NE oriented left-lateral strike-slip faults. These fault systems would accommodate the Nubia-Eurasia convergence by means of a block rotation mechanism, which generates fault-bounded crustal blocks that rotate clockwise at rates of $2\text{--}3^\circ/\text{Ma}$. On the basis of seismic tomography and seismicity data in the Gibraltar area, Calvert *et al.* [2000] and Gutscher [2004] suggested that subduction of a remnant oceanic slab west of Gibraltar, which was the main geodynamic process active during the Tertiary, is still active in the region and it is responsible for the largest earthquakes in the Gibraltar area. On the other hand, recent GPS data from the Rif chain indicate that the complex velocity field measured in this area can be explained by an active

¹Dipartimento di Scienze Geologiche, Università Roma Tre, Rome, Italy.

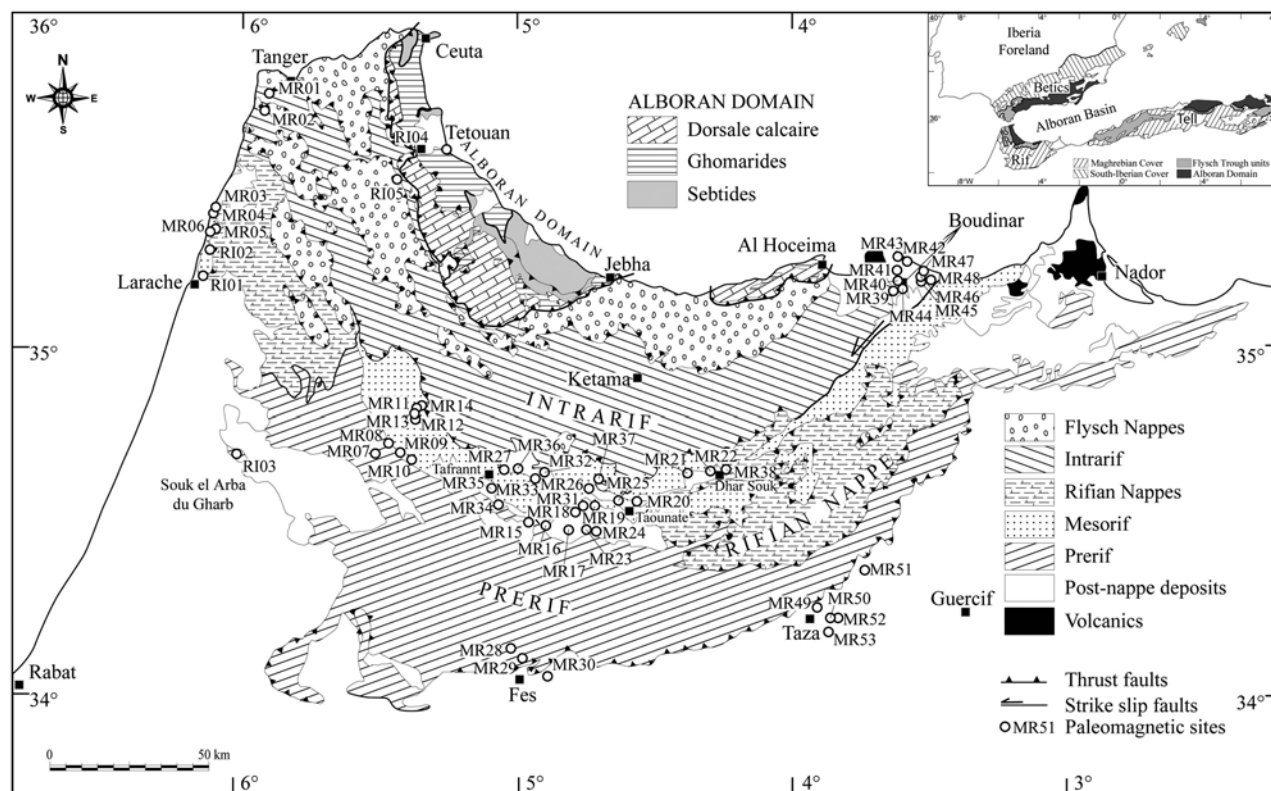


Figure 1. Schematic geologic map of the Rif chain (simplified from *Wildi* [1983] and *Chalouan et al.* [2001]). White circles and labels indicate paleomagnetic sites sampled in this study.

southwestward retreat of a remnant subducted slab in western Morocco [*Fadil et al.*, 2006].

[3] Most of the geodynamic models proposed to explain the tectonic evolution of the Gibraltar Arc and the Alboran Sea are based on paleomagnetic results that indicate large tectonic rotations in the opposite limbs of the chain, clockwise in the Betics and counterclockwise in the Rif (see *Platt et al.* [2003] for a recent review). These rotations are generally believed completed at the end of Tortonian [e.g., *Krijgsman and Garcés*, 2004], even though most of paleomagnetic data from the Gibraltar Arc come from Mesozoic rocks, whereas no data are available from Tertiary rocks in the Rif.

[4] In this study, in order to cover the lack of paleomagnetic information in Neogene deposits, a new paleomagnetic sampling was carried out in the Rif chain, in basins located in different tectonic domains along the chain. Paleomagnetic data from this study represent the first results from upper Miocene sedimentary rocks in the External zone of the Rif chain. Our results show that upper Miocene deposits from the Rif chain rotated counterclockwise, allowing for more precise definition of the time and the amount of paleomagnetic rotations in this part of the Gibraltar Arc. These data define a substantial rejuvenation of the age of rotations and represent a first-order constraint for the Neogene tectonic evolution of this sector of the Eurasia-Nubia plate boundary.

2. Geologic and Tectonic Setting of the Rif Chain

[5] The Rif chain is traditionally divided into three main structural domains: the Internal Rif, the Flysch domain and

the External Rif. These units form an arcuate mountain belt trending from NNW along the Atlantic coast to ENE in the eastern section (Figure 1). The Internal Rif corresponds to the Moroccan part of the Alboran Domain. It consists of metamorphic units forming the inner part of the Gibraltar Arc and the continental basement of the extensional Alboran Sea basin, and of nonmetamorphic units, such as the Ghomarides nappes and the “Dorsale” units [*Balanyá et al.*, 1997; *Comas et al.*, 1999]. The Internal Rif is juxtaposed against the Flysch nappes and Intrarif units through a thrust contact or, locally, through a left-lateral strike-slip fault (Jebha fault). The Maghrebien (Intermediate) Flysch nappes are mainly made up of Mesozoic to lower Miocene deep marine deposits that originated from an ocean or transitional crust-floored basin, which was located between the North African margin and the Internal Zones domain during the Mesozoic-Paleogene [*Durand-Delga et al.*, 2000; *Suter*, 1980; *Wildi*, 1983]. The Flysch nappes also include an uppermost nappe that is mainly made up of upper Oligocene–Aquitian coarse siliciclastic turbidites (Numidian nappes).

[6] The External Rif mostly consists of Mesozoic-Eocene, preorogenic sediments from the rifted continental margin of Africa and it is detached along the upper Triassic evaporitic red beds and thrust toward the Atlas-Meseta foreland. The External Rif is usually subdivided into the Intrarif, Mesorif, and Prerif domains, from a more internal (northward) to an external (southward) location [*Suter*, 1980]. These domains show sedimentary facies with a general trend from deep water (either terrigenous or pelagic) in the Intrarif to shallow water in the Prerif [*Durand-Delga et al.*, 1962]. Much of the Prerif

is buried beneath the Neogene to Recent sediments of the foreland basin and it is constituted by a chaotic mixture of Triassic evaporites and Mesozoic to lower Miocene marly rocks [Flinch, 1996; Wildi, 1983]. In places, the internal Prerif, Mesorif and Intrarif units are tectonically overlain by Mesozoic to Tertiary units, mainly coming from the Intrarif or the Flysch Domain [Crespo-Blanc and Frizon de Lamotte, 2006; Frizon de Lamotte et al., 2004; Platt et al., 2003]. These include the Rifian nappes, likely derived from the Mesorif or the external margin of the Intrarif (Figure 1).

[7] The different tectonic units that form the Rif chain are arranged in a complex fold and thrust architecture that is characterized by out-of-sequence and synchronous thrust propagation, which is responsible for most of the anomalous tectonic contacts recognized throughout the Rif chain [Frizon de Lamotte et al., 2004; Morley, 1992; Platt et al., 2003]. In the internal part of the chain, high-pressure (HP) metamorphic rocks are involved in the orogenic wedge, whereas the structural style of the external portion of the chain is debated, being supposed thin skinned [Platt et al., 2003] or thick skinned [Crespo-Blanc and Frizon de Lamotte, 2006; Favre, 1995; Michard et al., 2005]. The eastern boundaries of the different structural units are characterized by sinistral transpressive shear zones, such as the Jehba and Nekor faults [Leblanc and Olivier, 1984], which have been active mostly during the middle-late Miocene and constitute the lateral ramps of the internal thrust sheets [Chalouan et al., 2001; Frizon de Lamotte et al., 1991; Platt et al., 2003]. It is worth noting that the Jehba and the Nekor faults are parallel to the northeastern continuation of the Middle Atlas Shear Zone, which suggests the possibility that their location is inherited from an ancient structural fabric of the African foreland [Meghraoui et al., 1996].

[8] The timing of contractional deformation in the Rif has been defined in detail by tectonostratigraphic and seismic data that was collected from Miocene synorogenic sediments along the different sectors of the chain [Morley, 1992]. These sediments, deposited at the front of the orogenic wedge or on top of thrust units, define a general southwestward migration of compressional deformation that began in late Oligocene–early Miocene when contractional tectonics caused overthrust of the Alboran domain on top of the Flysch units. During early-middle Miocene, the front of the orogenic wedge reached the Flysch and Intrarif domains, as indicated by the onset of huge siliciclastic units deposited in foredeep and thrust top basins in these areas [Morley, 1988]. During the middle-late Miocene, the front of the Rif chain was located in the Prerif domain. At that time, the external foredeep basins were filled with huge olistostromes, analogous to those of the Guadalquivir foreland basin in the Betic chain, which indicated strong tectonic activity at the front of the Rif chain [Frizon de Lamotte et al., 2004].

[9] The outer front of the Rif chain appeared to be sealed by upper Miocene sediments along the Gharb plain, and in the Atlantic abyssal plain [Frizon de Lamotte et al., 2004; Meghraoui et al., 1996], which indicated that the main phases of nappe emplacement in the Gibraltar Arc halted during late Miocene. The progressive southwestward migration of contractional tectonics in the Rif chain was accompanied, during the early Miocene, by the onset of extensional processes affecting the inner part of the orogenic wedge and causing the

formation of the Alboran Sea [Comas et al., 1999]. Volcanism accompanied and postdated Neogene extension, with calc-alkaline, potassic and basaltic volcanism scattered across the eastern sector of the Alboran Sea and Rif chain [Duggen et al., 2003].

[10] From late Miocene onward, the westernmost Mediterranean area acted as a diffuse plate boundary between Africa and Eurasia. Contractional and strike-slip tectonic processes affected a wide region between the Alboran Sea and the Atlas chain and they were responsible for thrusting and folding of the upper Miocene postnappe basins in the Central Rif as well as of the folding and uplift of the upper Miocene and Pliocene sediments in the Rharb, Guercif, and Taza basins [Bernini et al., 2000; Frizon de Lamotte et al., 2004; Samaka et al., 1997; Sani et al., 2000; Tejera de Leon et al., 1995].

[11] Present-day tectonics in Morocco is mainly controlled by the convergence between Eurasia and Nubia plates, which move about 4 mm/a with a NW orientation according to GPS and to seismic data [Mc Clusky et al., 2003]. The recent 1994 and 2004 Al Hoceima earthquakes, which occurred along NNE oriented left-lateral and WNW oriented right-lateral strike-slip faults, respectively, indicate that active faulting is consistent with the plate motion vector determined by GPS and confirm a role for Nubia-Eurasia kinematics in present-day active deformation in the western Mediterranean [Biggs et al., 2006].

3. Previous Paleomagnetic Results and New Paleomagnetic Sampling

[12] Compared with other arcuate orogenic systems in the Mediterranean area, such as the Calabrian Arc for which detailed paleomagnetic studies have been carried out (for a recent review, see Cifelli et al. [2007]), the Rif chain lacks comprehensive paleomagnetic information, particularly from Neogene deposits. In the past years, paleomagnetic investigations were carried out in Mesozoic and Tertiary limestones in the Dorsale Calcaire of the Internal Rif [Platzman, 1992; Platzman et al., 1993]. Whereas most of the Jurassic and Cretaceous limestones carry stable remanent magnetization, no reliable results were obtained from Miocene rocks. Paleomagnetic data from six Jurassic sites (41 samples) and two lower Cretaceous sites (13 samples) indicated that significant rigid body rotations occurred in the Rif chain. According to Platzman [1992] and Platzman et al. [1993], these rotations were systematic, mainly counterclockwise (up to 100°), regional in extent and contributed to the shaping of the Betic-Rif curved orogenic system. Other paleomagnetic data come from the study by Platt et al. [2003], which investigated limestones of either middle to late Jurassic and of late Cretaceous age. From 35 study sites sampled around the External Rif, Platt et al. obtained reliable results from 18 sites (145 samples) of Lower Jurassic rocks. These results indicated quite consistent anticlockwise rotations of up to 135°. According to Platt et al., paleomagnetic results from Jurassic and Cretaceous rocks were certainly post-late Cretaceous and were probably associated with folding and thrusting during the early to middle Miocene. More recently, paleomagnetic studies have been carried out on Neogene basins of the Rif foreland for magnetostratigraphic investigations [Hilgen

et al., 2000; *Krijgsman and Garcés*, 2004; *Krijgsman et al.*, 1999; *Van Assen et al.*, 2004]. Paleomagnetic data from five magnetostratigraphic sections (302 samples) in Tortonian to Messinian deposits indicate that no major deflection from the north has occurred since the deposition of the sediments. On the basis of these results, *Krijgsman and Garcés* [2004] concluded that the Neogene basins of the Rif chain have not experienced any rotations about vertical axes since late Tortonian. The totality of data from Neogene deposits collected by *Krijgsman and Garcés* comes from the foreland domain; conversely, paleomagnetic data are completely missing for the Neogene sectors of the Rif chain itself.

[13] In order to fill the existing gap in paleomagnetic information and to further contribute to the reconstruction of the history of paleomagnetic rotations in the Rif chain through time, we focused our paleomagnetic sampling mostly on Neogene deposits. We selected sedimentary basins located in very different areas of the Rif, in order to obtain paleomagnetic data from structural domains that experienced different tectonic evolution during the Neogene. In particular, we sampled sediments in (1) upper Miocene extensional basins (Boudinar basin) which formed along the Mediterranean coast as a consequence of post-orogenic extension related to the opening of the Alboran Sea (MR39-48); (2) upper Tertiary foredeep and thrust top basins developed in the Rif chain during the Oligocene–middle Miocene and now included in the Rif orogenic wedge (RI01-02, RI05, MR01-06, MR07-14, MR28-29); (3) upper Miocene thrust top basins (Taouate-Tefrannt-Dhar Souk) which unconformably rest on top of Intrarif and Mesorif units of the Central Rif (MR15-27, MR31-38); and (4) the Taza-Fes upper Miocene foreland basin (RI03, MR30, MR49-53). Furthermore, we sampled one site (RI04) in the internal part of the Rif. The locations of the sampled areas are reported in Figure 1. In total, we sampled 58 sites, with 650 oriented samples that were almost homogeneously distributed along the Rif chain length (see Table S1 available in the auxiliary material).¹

[14] In the northern part of the Rif chain (structural domain 1), we sampled 10 sites from the Neogene post-nappe sediments of the Boudinar basin (MR39-48), a triangular-shaped depression filled by upper Miocene to Quaternary sedimentary deposits and bounded, in its southeastern edge, by the sinistral strike-slip Nekor fault. Sampling was carried out in Tortonian and Messinian marls that outcrop along the banks of major streams (Oued Amekrane and Oued Ichzar Si Salah) flowing into the Mediterranean Sea [*Guillemin and Houzay*, 1982].

[15] In the Oligocene–middle Miocene foredeep and thrust top basins (structural domain 2) a total of 19 sites were sampled. In the Flysch nappe, two sites were located in the Numidian Flysch deposits, one (MR01) was sampled along the Atlantic coast, close to Tanger city, and one (RI05) was south of the Tetouan city. The Numidian thrust sheet is predominantly composed of coarse upper Oligocene to lower Miocene turbidite sandstones. It overlays the (Intrarif) Tanger thrust sheet and appears to have a major out-of-sequence thrust at its base [*Morley*, 1988]. In the Intrarif deposits of the Tanger thrust sheet, four sites

(MR03-MR06) were taken in the Larache-Acilah area, along the Atlantic coast. Here, sampling was carried out in the upper Oligocene–lower Miocene Acilah sandstones unit, a turbidite sequence found at the leading edge of the Tanger thrust sheet [*Morley*, 1992]. Moreover, we sampled one site (RI02) in the Eocene-Oligocene shales and one in the Upper Cretaceous deposits (MR02), still within the Tanger thrust sheet. In the Mesorif, four sites (MR11-MR14) were sampled in the Burdigalian to Serravallian Zoumi sandstone thrust sheet unit [*Ben Yaich et al.*, 1989; *Morley*, 1988]. In the Prerif, a total of seven sites located in different tectonic units were sampled. One site (RI01) was sampled in the Larache area in the middle Eocene-Oligocene turbidites of the Sidi Mrait unit, which, together with the above mentioned Acilah sandstone sequence, represents the Tertiary foredeep sequences of the external zones of the northwestern Moroccan Rif [*Morley*, 1992]. Moving to the east, four sites (MR07-MR10) were sampled in the Ouz-zane nappe, another external flysch body that is Oligocene–early Miocene in age. Furthermore, two sites (MR28-29) were sampled in the upper Miocene Prerif sediments that are close to Fes.

[16] Detailed paleomagnetic sampling was performed in the Neogene intramontane Taouate-Tefrannt-Dhar Souk basins (structural domain 3), located in the central part of the Rif chain (Figure 1). These basins seal the boundary between the Intrarif and the Mesorif tectonic units, as they overlay the tectonic boundary between the Intrarif tectonic nappes and the Mesorif units located north and south of the basins, respectively. The Neogene basins of the central Rif are interpreted as thrust top basins formed during the southward propagation of the Prerif units [*Samaka et al.*, 1997; *Tejera de Leon et al.*, 1996]. The sedimentary filling of the basins consisted of several sedimentary cycles, evolving from continental to the marine environment [*Wernli*, 1988]. The continental sedimentary sequence began in the Tortonian with sandstones and conglomerates, which unconformably rest on top of Meso-Cenozoic units of the Rif chain. Continental deposits progressively evolved to marine conditions during the late Tortonian and early Messinian and progressed toward open marine environments, when clay sediments were deposited along the entire area [*Wernli*, 1988]. Each of the Taouate-Tefrannt-Dhar Souk basins presents a synform structure framed by NE-SW, E-W, and WNW-ESE faults [*Ait Brahim and Chotin*, 1989]. A total of 21 sites (MR16-27 and MR31-38) were sampled in the marine marls and clays outcropping in the basins. The ages of the sampled sites range from late Tortonian to Messinian [*Tejera de Leon et al.*, 1995; *Wernli*, 1988].

[17] In the foreland domain (structural domain 4), from west to east, one site (RI03) was sampled in the upper Miocene Gharb-Mamora basin marls, one site (MR30) in the upper Miocene deposits of the Fes basin and five sites (MR49-53) in the Taza-Guercif upper Miocene deposits.

[18] Finally, we sampled one site (RI04) in the Tetouan basin, where small strips of upper Miocene deposits outcrop along the coast.

[19] Ten to fifteen 2.5 cm diameter cores were drilled at each site with a gasoline-powered drill and were oriented in situ with a magnetic compass. Cores were taken as far as possible from local tectonic features (faults, slumps, creep,

¹Auxiliary materials are available in the HTML. doi:10.1029/2007JB005271.

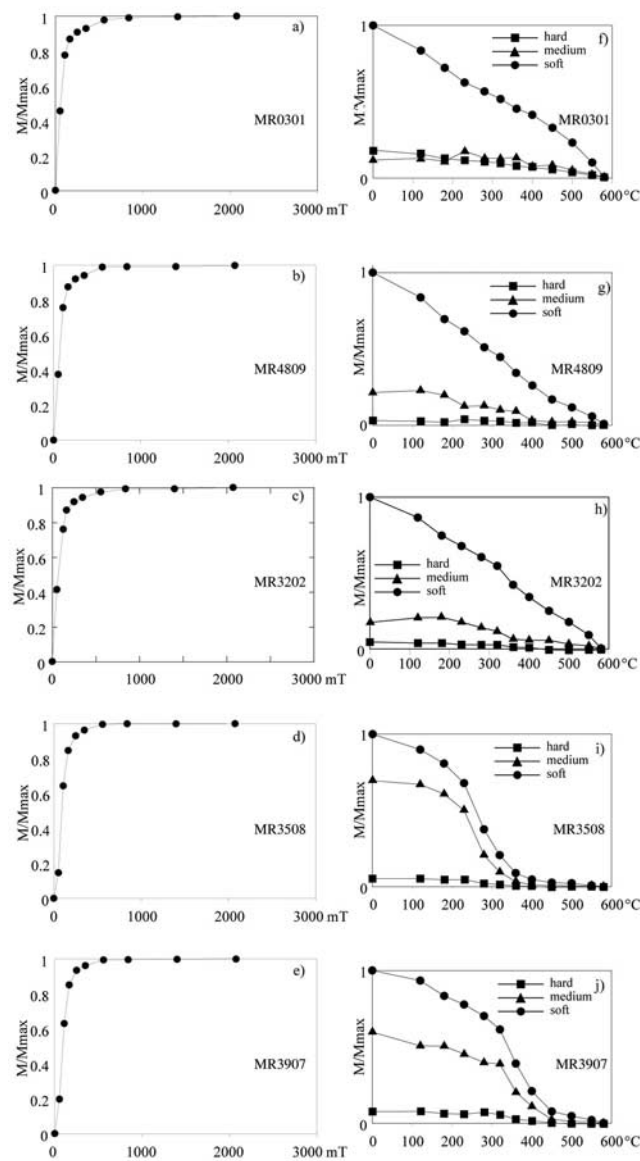


Figure 2. Magnetic mineralogy of the analyzed samples. (a–e) IRM acquisition curves showing the prevalence of low-coercivity in the analyzed samples. (f–j) Thermal demagnetization curves of a three-component (hard, medium, soft) IRM [Lowrie, 1990] are shown for magnetite bearing samples (Figures 2f–2h), iron sulphides bearing samples and samples containing both iron sulphides (Figure 2i), and magnetite (Figure 2j).

etc.) and from different stratigraphic levels in order to average the secular variation of the geomagnetic field.

4. Paleomagnetic Analysis

4.1. Magnetic Mineralogy and Demagnetization of the Natural Remanent Magnetization

[20] Paleomagnetic analyses were carried out at the paleomagnetic laboratory of Roma TRE University and at the Alpine Laboratory of Paleomagnetism (ALP) of Peveragno, using standard methods. Magnetic mineralogy was analyzed for one sample per site. First, isothermal remnant

magnetization (IRM) was studied by applying a stepwise increasing magnetic field along the sample *z* axis and by measuring the remanent magnetization after each step with a JR6a spinner magnetometer. The applied field was up to 2.1 T and was produced by a pulse magnetizer. The unblocking temperature spectra of the samples were then studied by thermally demagnetizing a composite IRM [Lowrie, 1990]. Before demagnetization, magnetic fields of 2.1, 0.6 and 0.12 T was applied along the *z*, *y*, and *x* axes, respectively, with a pulse magnetizer.

[21] Low-coercivity ferrimagnetic minerals were identified in the totality of the analyzed rocks (Figures 2a–2e). For some specimens, the maximum unblocking temperature was about 580°C, indicating that magnetite is the main magnetic carrier (Figures 2f–2h). In other specimens, the maximum unblocking temperatures are in the range of 320–360°C, which suggests that the magnetic mineralogy is dominated mainly by iron sulphides (Figure 2i). In some other sites containing iron sulphides, a small amount of remanence was still present after 400°C, indicating that high-temperature magnetization is carried by magnetite (Figure 2j). High-coercivity magnetic carriers were not identified in the analyzed specimens.

[22] The natural remanent magnetization (NRM) of specimens was analyzed by both progressive stepwise thermal demagnetization and stepwise alternating field demagnetization, according to preliminary results obtained from pilot specimens from each site. Magnetic cleaning was stopped when the NRM reached the sensitivity level of the instrument or when a random change of the paleomagnetic direction appeared. Demagnetization data were analyzed using orthogonal vector diagrams (Figure 3) and the directions of the remanence components were estimated using principal component analysis [Kirschvink, 1980]. In some cases, samples were too weakly magnetized (NRM values about 50×10^{-6} A/m) to allow for reliable, complete, stepwise demagnetization. For most of the AF demagnetized samples, after removal of small viscous components by 10–20 mT, a well-defined ChRM was isolated and demagnetized at 60–90 mT (Figures 3e–3f). For thermally demagnetized samples, a viscous component was generally recognized, which was removed at about 120–180°C. Afterward, a ChRM was generally isolated, and specimens were completely demagnetized at 360–400°C (Figures 3g–3i) or, rarely, at 450–530°C (Figure 3j), confirming the presence of iron sulphides and titanomagnetite, respectively, as main magnetic carriers. Most of the specimens yield a maximum angular deviation (MAD) < 15°, with most of them (about 85%) yielding (MAD) < 10°. Samples yielding MAD > 17.5° were rejected and were not considered in further analyses.

4.2. Paleomagnetic Directions

[23] Site-mean paleomagnetic directions were calculated using Fisher's [1953] statistics on 29 sites where only ChRMs were isolated, whereas the *McFadden and McElhinny* [1988] method was used on three sites where both ChRMs and remagnetization circles were observed. In 21 sites, well-defined ($\alpha_{95} < 10.0^\circ$) ChRMs were isolated, while in another eight sites, the ChRM was less defined ($\alpha_{95} < 15.0^\circ$). In three sites, the ChRMs were poorly defined ($\alpha_{95} > 15.0^\circ$), but they were coherent with the other sites from the same

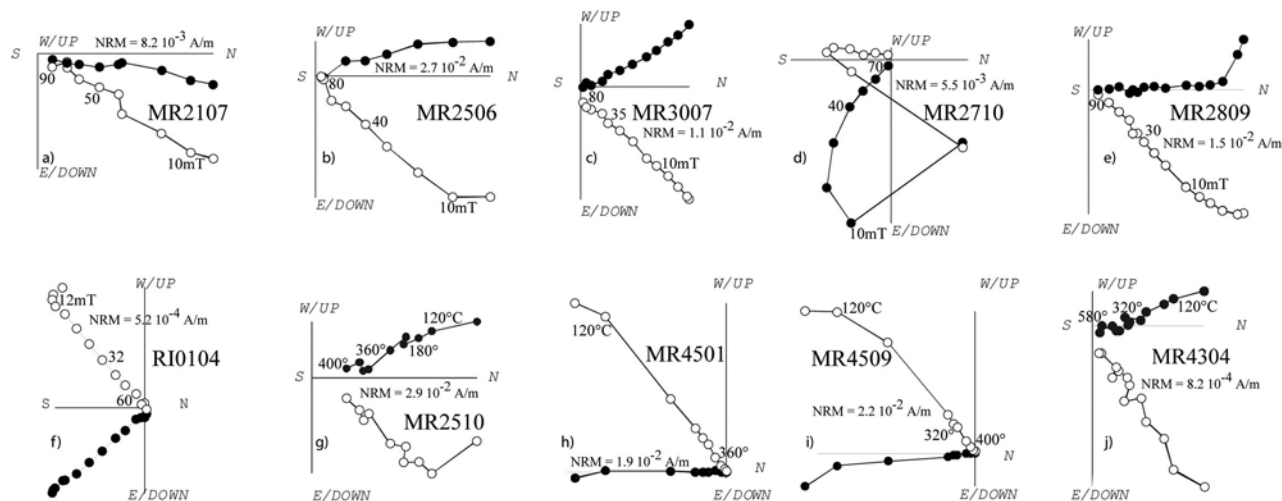


Figure 3. Vector component diagrams (Zijderveld diagrams, in geographic coordinates) for the progressive (a–f) AF and (g–j) thermal demagnetization of representative samples. Demagnetization step values are in mT and degrees Celsius, respectively. Open and solid symbols represent projection on the vertical and horizontal planes, respectively.

basins and, therefore, were considered in further tectonic interpretations. In total, we obtained reliable sites with mean directions from 32 sites (Table 1), as described below.

[24] In the Boudinar basin (structural domain 1), from the 10 sampled sites (MR39–48), reliable paleomagnetic results have been obtained from six sites. Both normal (one site) and reverse (five sites) polarities have been observed (reversal test is indeterminate according to *McFadden and McElhinny* [1990]). However, the one site with a normal polarity has a ChRM very close to the present-day geomagnetic geocentric axial dipole field (GAD) for Morocco, suggesting that this site has been recently remagnetized. For this reason, site MR43 was not considered in further tectonic interpretation (Table 1). Because of the almost subhorizontal bedding attitude at the sampled sites (Table 1), the fold test was inconclusive and indeterminate according to *McFadden* [1990]. However, at the basin scale the mean paleomagnetic direction was better grouped after ($D = 181.7^\circ$, $I = -56.6^\circ$, $K = 61.4$, $\alpha_{95} = 8.6$) as compared to before tectonic correction ($D = 181.9^\circ$, $I = -58.4^\circ$, $K = 37.6$, $\alpha_{95} = 11.1$). Moreover, when we apply an inclination-only fold test inclination values are better grouped after ($\alpha_{95} = 11.1^\circ$) than before tectonic correction ($\alpha_{95} = 14.7^\circ$), suggesting that the isolated ChRM was acquired before the tilting of the bedding (Figure 4a).

[25] In the western and central parts of the Rif chain, sites collected from the Rifian nappes and the Prerif Units (structural domain 2) showed poor magnetization and poorly defined paleomagnetic directions. Most of the sites were too weakly magnetized or showed unstable behavior during thermal and/or AF demagnetization. From the 19 sites sampled in this part of the Rif, consistent results were obtained from six sites. Among these, three sites gave reliable paleomagnetic results from the Acilah-Larache area: site RI01 in the Oligocene-Eocene shales from the Prerif thrust sheet in the Larache area and sites MR03 and MR06 from the upper Oligocene–lower Miocene Acilah sand-

stones from the Tanger thrust unit. After tectonic correction, these sites showed consistent paleomagnetic declination (Table 1). In site RI01, samples with normal and reverse polarities (with almost antipodal directions) have been observed (reversal test is indeterminate, according to *McFadden and McElhinny* [1990]), which suggest that the demagnetization procedure was able to remove recent remagnetization and could isolate the primary ChRM. All of these sites were characterized by counterclockwise rotations (about 25° on average). The other three reliable sites were sampled in the western Numidian nappe (RI05) in the upper Miocene Prerif units that were north of Fes city (MR28) and southwest of Zoumi village (MR08) (Figure 1). These three sites showed normal polarity, which could indicate a recent magnetic overprint of these sites. However, in geographic coordinates their directions are significantly far from the GAD present-day field for Morocco, which suggest a primary origin of the isolated ChRM. After tectonic correction, the three sites showed coherent north-west oriented declinations (Table 1).

[26] From the 21 sites sampled in the Taouate-Tefranth-Dhar Souk thrust top basins (MR15–27, MR31–38) (structural domain 2), reliable paleomagnetic results were obtained from 12 sites that were almost homogeneously distributed from the Tefranth basin in the west to the Dhar Souk basin in the east. Both normal and reverse polarities were observed and they exhibited almost antipodal mean directions (reversal test is, however, indeterminate according to *McFadden and McElhinny* [1990]). Sites with normal polarity show a ChRM direction that is far from the present-day geomagnetic geocentric axial dipole field (GAD) and indicates that there was not a recent magnetic overprint for these sites (Table 1). Furthermore, at the basin scale the mean paleomagnetic direction is better grouped after ($D = 338.2^\circ$, $I = 44.2^\circ$, $K = 19.7$, $\alpha_{95} = 10.0$), than before tectonic correction ($D = 343.7^\circ$, $I = 33.0^\circ$, $K = 8.6$, $\alpha_{95} = 15.7$) (Figure 4b). The data pass the *McFadden* [1990] fold test at the 99% confidence level ($\xi_{\text{in situ}} = 7.459$; $\xi_{\text{unfolded}} = 2.185$;

Table 1. Paleomagnetic Directions From the Rif Chain^a

Sites	Geographic Coordinates	Age	n1, n2/N	D _{BTC}	I _{BTC}	k	α_{95}	D _{ATC} ± δ D	I _{ATC}	k	α_{95}	S ₀
<i>Structural Domain 1: Postnappes Basin (Boudinar Basin)</i>												
MR39	35°08'40"N, 03°39'31"W	upper Tortonian-Messinian	14, 0/14	166.2	-41.6	116.6	3.7	170.5 ± 7	-59.3	116.6	3.7	157, 18 ^b
MR41	35°12'05"N, 03°35'44"W	upper Tortonian-Messinian	12, 0/12	182.2	-60.1	30.3	7.7	182.2 ± 15	-60.1	30.3	7.7	0, 0
MR42	35°13'00"N, 03°33'55"W	upper Tortonian-Messinian	9, 0/9	166.0	-66.0	54.9	7.0	166.0 ± 15	-56.0	54.9	7.0	346, 10 ^b
MR43 ^c	35°13'55"N, 03°36'28"W	upper Tortonian-Messinian	11, 0/11	353.0	55.3	112.5	4.3	342.9 ± 6	45.3	112.5	4.3	308, 13
MR45	35°10'24"N, 03°32'45"W	upper Tortonian-Messinian	13, 0/13	182.5	-48.4	285.6	2.5	186.9 ± 3	-39.5	285.6	2.5	32, 10
MR46	35°11'22"N, 03°32'27"W	upper Tortonian-Messinian	9, 0/9	206.6	-67.3	26.2	10.2	197.4 ± 20	-60.6	26.2	10.2	348, 8
Basin mean direction				181.9	-58.4	37.6	11.1	181.7 ± 14	-56.6	61.4	8.6	
<i>Structural Domain 2: Rifian Nappes and the Pre-Rif Units</i>												
RI01	35°11'22"N, 06°03'46"W	Oligocene-Eocene	6, 0/6 r/n	325.4	41.2	41.8	10.5	326.0 ± 19	58.2	41.8	10.5	144, 17
MR03	35°27'57"N, 06°02'27"W	upper Oligocene-lower Miocene	7, 0/7	339.8	5.9	12.5	17.8	339.9 ± 19	21.0	12.5	17.8	161, 15
MR06	35°21'56"N, 06°02'34"W	upper Oligocene-lower Miocene	7, 0/7	332.1	47.6	35.5	13.0	330.8 ± 15	30.8	35.5	13.0	348, 15
MR08	34°45'12"N, 05°27'01"W	upper Oligocene-lower Miocene	7, 0/7	332.8	35.1	76.3	7.0	285.3 ± 11	50.8	76.3	7.0	202, 48
RI05	35°25'40"N, 05°21'46"W	Oligocene-Miocene	7, 0/7	339.8	53.6	49.7	8.6	330.1 ± 16	58.2	49.7	8.6	210, 8
MR28	34°10'04"N, 05°02'22"W	upper Miocene	13, 0/13	344.8	39.9	16.0	10.7	349.4 ± 25	64.7	16.0	10.7	159, 25
<i>Structural Domain 3: Thrust Top Basins (Taounate-Tefrannt-Dhar Souk Basins)</i>												
MR17	34°29'29"N, 04°49'22"W	upper Tortonian-Messinian	7, 0/7	176.4	-4.7	17.1	15.0	174.6 ± 16	-20.8	17.1	15.0	202, 18
MR19	34°32'56"N, 04°43'04"W	upper Tortonian-Messinian	16, 0/16	339.3	30.8	34.1	6.4	332.5 ± 8	40.3	34.1	6.4	200, 13 ^b
MR20	34°34'22"N, 04°34'26"W	upper Tortonian-Messinian	9, 0/9	313.5	55.6	55.6	7.0	316.0 ± 10	47.8	55.6	7.0	329, 8
MR21	34°38'41"N, 04°23'27"W	upper Tortonian-Messinian	9, 0/9	7.7	37.7	73.4	6.0	305.1 ± 10	53.8	73.4	6.0	233, 55 ^b
MR23	34°29'54"N, 04°45'34"W	upper Tortonian-Messinian	8, 1/9	352.0	13.8	63.5	6.6	351.1 ± 10	48.8	63.5	6.6	174, 35
MR24	34°29'07"N, 04°44'09"W	upper Tortonian-Messinian	10, 1/11	159.9	-21.3	17.5	11.3	178.2 ± 15	-42.0	17.5	11.3	114, 35
MR25	34°33'56"N, 04°37'30"W	upper Tortonian-Messinian	13, 0/13	344.1	43.3	33.0	7.0	355.3 ± 10	48.7	33.0	7.0	106, 12
MR27	34°39'44"N, 05°03'49"W	upper Tortonian-Messinian	10, 0/10	111.3	2.6	33.0	8.5	120.8 ± 11	-43.2	33.0	8.5	88, 51
MR31	34°32'52"N, 04°46'59"W	upper Tortonian-Messinian	10, 0/10	354.4	22.5	37.8	8.0	359.1 ± 11	44.5	37.8	8.0	159, 23 ^b
MR32	34°39'09"N, 04°54'10"W	upper Tortonian-Messinian	12, 0/12	327.5	43.0	36.1	7.3	338.4 ± 8	20.7	36.1	7.3	11, 28
MR35	34°37'53"N, 05°05'15"W	upper Tortonian-Messinian	5, 0/5	174.7	-43.0	11.1	24.0	147.1 ± 35	-47.4	11.1	24.0	242, 27
MR38	34°39'28"N, 04°16'16"W	upper Tortonian-Messinian	8, 0/8	28.0	55.2	39.9	8.9	347.9 ± 15	52.1	39.9	8.9	284, 29 ^b
Basin mean direction				343.7	33.0	8.6	15.7	338.2 ± 13	44.2	19.7	10	
<i>Structural Domain 4: Foreland Basins (Gharb, Fez, and Taza Basins)</i>												
MR49	34°15'22"N, 03°57'30"W	Messinian	11, 0/11	354.3	53.6	17.0	10.4	1.1 ± 15	45.3	17.0	10.4	33, 10 ^b
MR50	34°14'03"N, 03°54'51"W	Messinian	12, 0/12	351.5	39.9	32.2	7.8	339.8 ± 13	53.7	32.2	7.8	206, 18
MR51	34°21'49"N, 03°45'41"W	Messinian	10, 0/10	187.8	-48.8	66.3	6.0	187.1 ± 10	-53.8	66.3	6.0	194, 5 ^b
MR52	34°14'12"N, 03°54'14"W	Messinian	9, 0/9	5.0	41.4	19.7	11.9	358.8 ± 16	41.3	19.7	11.9	273, 7 ^b
MR53 ^c	34°09'33"N, 03°54'43"W	Messinian	8, 2/10	3.0	44.6	224.5	3.3	41.0 ± 6	55.9	224.5	3.3	131, 32
MR30	34°01'49"N, 04°52'51"W	upper Miocene	8, 0/8	341.1	41.3	81.8	6.2	344.4 ± 7	33.4	81.8	6.2	11, 9
RI03	34°41'25"N, 05°59'54"W	upper Miocene	6, 0/6	281.4	46.8	46.3	9.9	341.7 ± 16	53.1	46.3	9.9	48, 56 ^b
<i>Internal Rif</i>												
RI04	35°34'54"N, 05°15'22"W	upper Miocene	3, 0/3	325.5	25.0	110.6	11.8	328.6 ± 17	45.5	110.6	11.8	135, 21

^aThe n1, n2/N are number of stable directions and number of great circles/total number of studied samples at a site; D, I are site-mean declinations and inclinations calculated before (D_{BTC}, I_{BTC}) and after (D_{ATC}, I_{ATC}) tectonic correction; k and α_{95} are statistical parameters after Fisher [1953]; S₀ is bedding attitude (azimuth of the dip and dip values); r/n indicates sites characterized both by samples with reversal and normal polarity. Errors for declination values (\pm) are calculated respect to the north ($\text{err} = \alpha_{95}/(\cos I)$), according to Demarest [1983].

^bDeduced by AMS tensor.

^cSites not considered in further tectonic interpretation (not reported in Figure 5; see text for details).

$\xi_{99\%} = 5.624$). When we apply an inclination-only fold test inclination values are better grouped after ($\alpha_{95} = 5.9^\circ$) than before tectonic correction ($\alpha_{95} = 9.9^\circ$). The presence of both normal and reverse polarities and the positive fold tests indicate a pretilting age for the isolated component.

[27] In the foreland basin (structural domain 4), we were able to isolate well-defined ChRMs in seven sites from the Rharb (RI03), Fes (MR30) and Guercif-Taza (MR49-53) sedimentary basins. Sites from both the Rharb and Fes basins show normal polarity and northwestern declination when reported to stratigraphic coordinates and their directions (in geographic coordinates) were far from the GAD present-day field for Morocco, which indicate that the isolated ChRMs for these sites are not due to recent magnetic overprint. In the Guercif-Taza basin, we obtained well-defined directions

from five sites. Only one site (MR51) had a ChRM with a reverse magnetic polarity, whereas all of the other sites exhibited normal polarity for the isolated ChRMs. However, site MR53, which had an anomalous northeastern direction after tectonic correction, was very close to the present-day GAD magnetic field for Morocco in geographic coordinates, which suggests that this site was recently magnetically overprinted. For this reason, this site was not used in further tectonic interpretation. When sites from the Taza basin are considered together, they show a better grouping before tectonic correction (D = 359.6°, I = 46.0°, K = 87.9, $\alpha_{95} = 9.9^\circ$) than after tectonic correction (D = 356.9°, I = 48.8°, K = 60.1, $\alpha_{95} = 11.1^\circ$) (Figure 4c). Both the fold test [McFadden, 1990] and the reversal test [McFadden and McElhinny, 1990] are indeterminate. The best grouping of data is obtained at

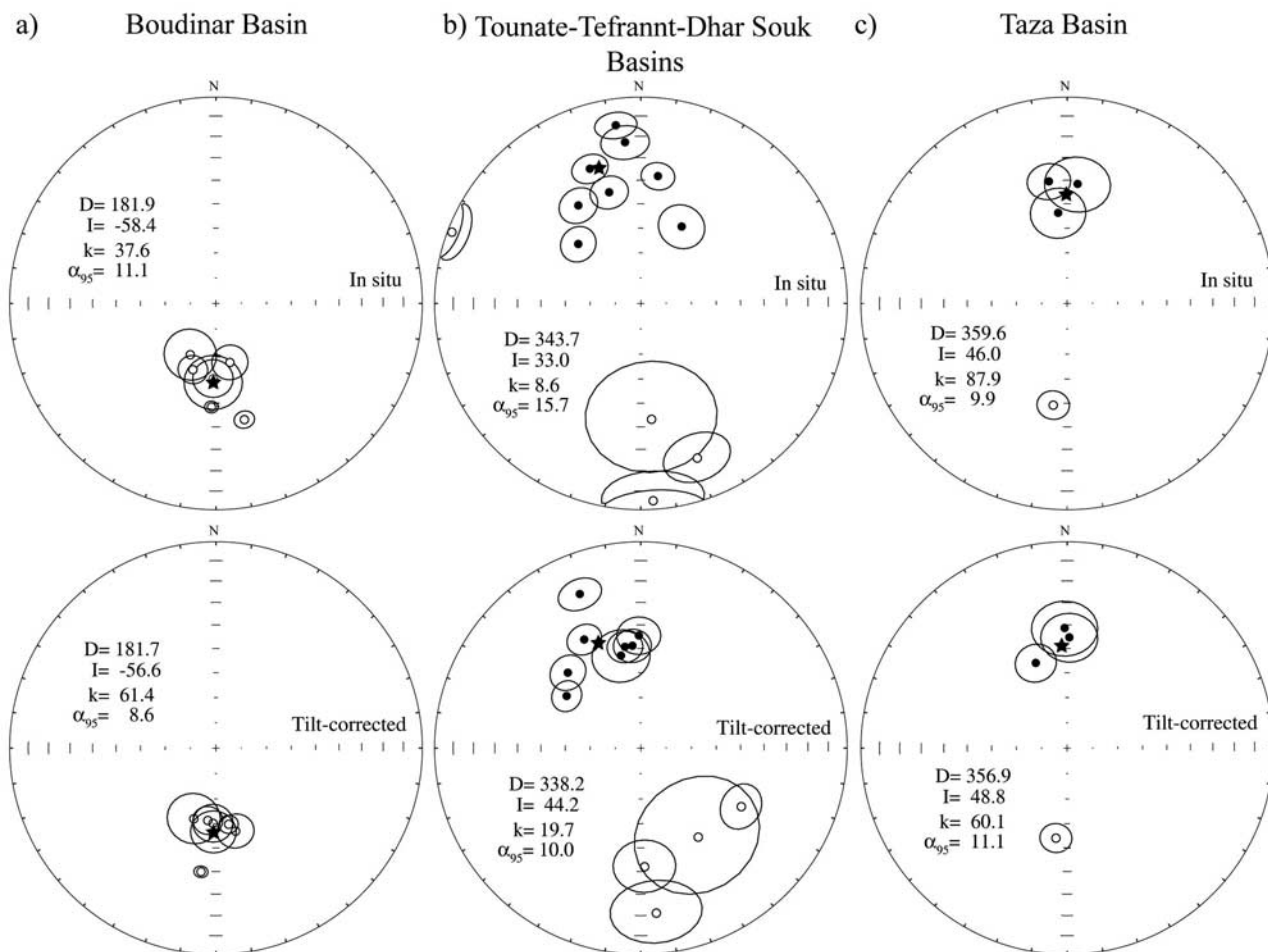


Figure 4. Equal-area projection of the site-mean directions from (a) Boudinar basin, (b) Tounate-Tefrannt-Dhar Souk basins, and (c) Taza Basin. White and black symbols represent projection onto upper and lower hemisphere, respectively. Ellipses are the projections of the α_{95} cone about the mean directions.

60% of complete unfolding which, however, has little meaning given the almost subhorizontal bedding attitude in most of the sites. Furthermore, when we apply an inclination-only fold test inclination values are better grouped before ($\alpha_{95} = 4.4^\circ$) than after tectonic correction ($\alpha_{95} = 6.9^\circ$). For these reasons we cannot conclusively exclude that recent magnetic overprints remain in some sites from the Taza basin. This casts some doubt on the reliability of the isolated ChRMs for sites from this basin.

[28] Finally, in the Internal Rif units, we obtained a reliable result from one site (RI04) from upper Miocene clay sediments in the Tetouan basin. This site had a normal polarity and a northwest oriented declination (Table 1).

5. Discussion

5.1. Analysis of Paleomagnetic Rotations

[29] In Figure 5, we report paleomagnetic data from this study and from previously published results on the Rif chain [Hilgen *et al.*, 2000; Krijgsman and Garcés, 2004; Krijgsman *et al.*, 1999; Platt *et al.*, 2003; Platzman *et al.*, 1993; Van Assen *et al.*, 2004]. In the following discussion, we distinguish results obtained from Oligocene–middle Miocene

rocks, which reflect the main phases of nappe emplacement of the Rif chain, from results obtained from upper Miocene deposits, which record the latest phases of thrusting and folding in the Rif chain and the contractional episodes related to the Africa-Eurasia convergence.

[30] In the Rif orogenic wedge, previous results were obtained exclusively from Mesozoic rocks [Platt *et al.*, 2003; Platzman, 1992; Platzman *et al.*, 1993]. These data indicate that large vertical axis rotations occurred in the Internal Zone as well as in the External zone. In the Internal Zone units, Platzman [1992] and Platzman *et al.* [1993] found large and quite variable rotations about vertical axes. Most of the tectonic rotations were counterclockwise (up to 127°), except for the area of Tetouan, where clockwise rotations (up to 123°) were measured (Figure 5). In the External Rif units, a large amount of counterclockwise rotations (up to 137°) were measured in Mesozoic rocks, mostly from the central and eastern parts of the chain (Figure 5). Our paleomagnetic data in the External Rif units come from Oligocene–middle Miocene rocks, with the exception of site MR28, which was sampled in upper Miocene deposits. These deposits show counterclockwise rotations ranging from about 25 degrees along the western-

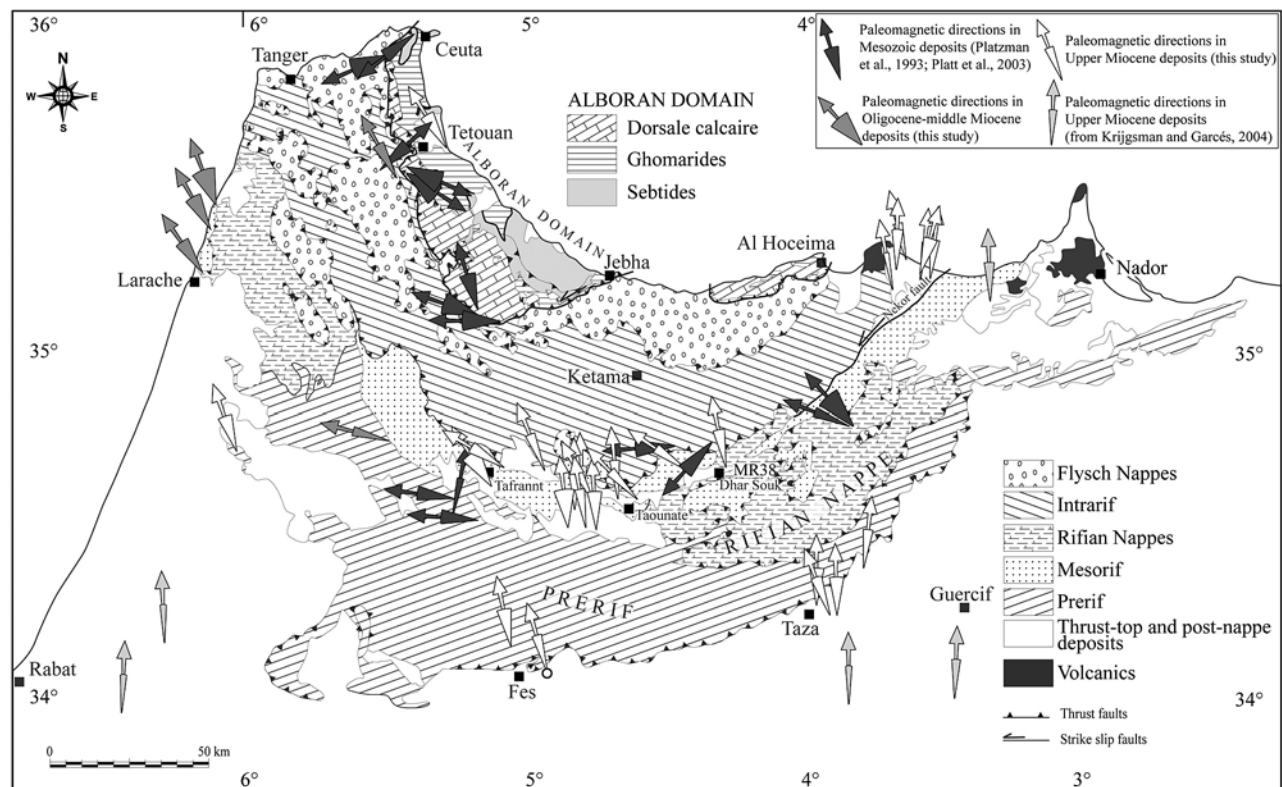


Figure 5. Paleomagnetic declinations (and relative confidence limits) from this study and from previous published results on the Rif chain. For Mesozoic rocks sampled by *Platzman et al.* [1993], rotations and confident limits were calculated by comparing paleodirections to the coeval reference directions of the African foreland from *Besse and Courtillot* [2002] according to *Demarest* [1983].

most External Rif units (Larache-Acilah region) to about 70° in the southwestern part of the chain (Figure 5). This may indicate that the central eastern part of the Rif chain underwent larger counterclockwise rotations with respect to the western part of the chain, which shows N-S trending that is almost perpendicular to the sense of tectonic transport deduced by structural data.

[31] Paleomagnetic data from upper Miocene deposits indicate a more complex distribution of tectonic rotations that was strongly dependent on the structural location of the sampled units. Magnetostratigraphic studies carried out in the Taza and Gharb foreland basins and in the postnappe Melilla basin indicate that the Tortonian-Messinian deposits were not affected by vertical axis rotations [*Hilgen et al.*, 2000; *Krijgsman and Garcés*, 2004; *Krijgsman et al.*, 2004; *Van Assen et al.*, 2004]. In this study, paleomagnetic data from late Miocene were collected in postnappe, thrust top, and foreland basin deposits (Table 1 and Figure 5). Data from the Taza foreland basin are consistent with the paleomagnetic results of *Krijgsman and Garcés* [2004] obtained in the same basin, which is located to the south of the outer front of the chain (Figure 5). In this basin, the paleomagnetic mean direction at the basin scale indicates that upper Miocene deposits did not undergo tectonic rotation (Figure 4). Similar directions are observed in the postnappe Boudinar basin, which is located at the northern edge of the Rif. In this area, the basin mean paleomagnetic

direction indicates that no tectonic rotations occurred after late Tortonian-Messinian (Figure 4).

[32] A different rotational pattern was observed in the thrust top Taouate-Tefrannt-Dhar Souk basins, which rest on top of the Meso and External Rif units, and in the more external part of the Prerif nappe (Figure 1). In the upper Tortonian-Messinian sedimentary units sampled in these basins, approximately $20^\circ \pm 13^\circ$ counterclockwise rotations were observed (Figures 4 and 5). These paleomagnetic results, which represent the first data gathered in upper Miocene sediments from the Rif orogenic wedge, suggest that counterclockwise rotations, previously measured in the Mesozoic units of the Rif chain, extended into the upper Miocene units of the chain, which indicates that the curvature of the Rif Arc was not completely achieved at that time.

5.2. Tectonic Implications of Paleomagnetic Results

[33] The geographic distribution and the timing of paleomagnetic rotations derived from this study, together with previously published data, evidence two main points: (1) counterclockwise rotations were only measured in the Rif orogenic wedge, whereas neither the postnappe extensional basins along the Mediterranean coast nor the foreland basin to the south show paleomagnetic rotations; and (2) counterclockwise rotations, previously measured only in Mesozoic units in the Rif chain, have also been measured in Oligocene–middle Miocene units, and they continued during the late Miocene. These two considerations give some important constraints for the reconstruction of the

Tertiary to present-day tectonic evolution of the Rif chain. Counterclockwise rotations in the Rif have been extensively measured in the different tectonic units that form the chain. The amount of counterclockwise rotations is strongly dependent on the age and the structural position of the sampled units, ranging from up to 127° in Mesozoic units from the Intrarif, to $30\text{--}40^\circ$ in the Oligocene–middle Miocene sediments in the Mesorif units along the western part of the chain, to about $20^\circ \pm 13$ in average in the upper Miocene thrust top basins in the central portion of the chain (Figure 5). At the same time, no rotations have been observed in either the upper Miocene foreland basins to the south or in the upper Miocene postnappe basins to the north. This pattern of paleomagnetic rotations indicates that vertical axis rotations are confined to the Rif orogenic wedge and that they occurred during the main phases of compressional deformation, together with the emplacement of the thrust units and with the progressive migration of the orogenic front and foredeep basins [Frizon de Lamotte et al., 2004]. It is worth noting that paleomagnetic rotations in the Betics, which forms the northern arm of the Gibraltar Arc, mirror those measured in the Rif, as clockwise rotations have been measured in Mesozoic to upper Miocene deposits within the Betic chain, whereas the upper Miocene Guadalquivir foreland basin does not exhibit rotations [Krijgsman and Garcés, 2004; Mattei et al., 2006].

[34] Huge and opposite vertical axis rotations along the two arms of the arc have been systematically measured in most of the orogenic arcs, whose formation characterizes the Tertiary tectonic evolution of the Mediterranean region [e.g., Lonergan and White, 1997; Kissel and Laj, 1988; Speranza et al., 1997]. In particular, a pattern of paleomagnetic rotations very similar to that observed in the Gibraltar Arc has been recognized in the Calabrian Arc, where large and opposite paleomagnetic rotations have been measured in the orogenic wedge, while no rotations have been registered on the Adriatic and African foreland basins [Cifelli et al., 2007; Mattei et al., 2006, 2007; Scheepers, 1992; Speranza et al., 1999]. In the Gibraltar area, the progressive curvature of the arc was achieved during the Neogene as a consequence of the progressive retreat of a narrow subducting slab, which induced arc migration and extension in the lithosphere of the overriding plate [Frizon de Lamotte et al., 1991; Faccenna et al., 2004; Gutscher et al., 2002]. Accordingly, paleomagnetic data suggest that the present-day curvature of the Gibraltar Arc was achieved through opposite rotations in the Betics and in the Rif chains, which continued during the late Miocene.

[35] Paleomagnetic data are not able to provide an upper temporal boundary for measured tectonic rotations, as no data from Plio-Pleistocene units are available from the Rif chain. Recent GPS data suggest that an independent, small, fault-bounded crustal block is moving southwestward, relative to Nubia, in central Rif. This motion has been tentatively interpreted to be the result of rollback of a narrow slab of delaminated continental lithosphere [Fadil et al., 2006], even though active west directed rollback of an east dipping slab, which should cause a westward motion of Gibraltar relative to Africa, is inconsistent with the well-defined eastward motion of GPS sites observed in northwestern Morocco [Mc Clusky et al., 2003]. This leaves the question of active subduction beneath the Gibraltar Arc unanswered. The

regional velocity field in the western Mediterranean suggests an active oblique convergence between Nubia and Iberia, with a right-lateral component of motion [Fadil et al., 2006]. In the northern Rif, NE-SW oriented left-lateral strike-slip faults and E-W oriented right-lateral fault cut obliquely across the chain and control the present-day active tectonics in the region. They are responsible for the largest earthquakes registered in this area [Akoglu et al., 2006; Biggs et al., 2006; Stich et al., 2006]. Some authors suggest that deformation mechanisms in the Gibraltar Arc changed from subduction-related tectonic processes to strike-slip deformation since late Miocene, with strike-slip faulting overlapping or postdating the bending process [e.g., Meghraoui et al., 1996]. Accordingly, $2\text{--}3^\circ/\text{Ma}$ of tectonic rotation should be associated with a block rotation mechanism related to strike-slip tectonics [Meghraoui et al., 1996]. This mechanism should allow for the Nubia-Iberia oblique convergence, producing a total of $10^\circ\text{--}15^\circ$ of clockwise rotations of the different rigid blocks of the northern Rif. However, in the Internal Rif, paleomagnetic results indicate the absence of tectonic rotations related to motion along the strike-slip zones (Figure 5). This suggests either that the rate of rotation is less than suggested by Meghraoui et al. [1996], producing tectonic rotations which correspond to the intrinsic degree of confidence of many paleomagnetic results [Butler, 1992], or that the initiation of the strike-slip regime in the Rif is younger than is generally believed.

6. Conclusions

[36] In this paper, new paleomagnetic data from the Rif chain have been presented. Paleomagnetic results from the upper Miocene deposits in the External Rif represent the first data gathered in upper Miocene sediments from the Rif orogen. Whereas no rotations have been measured in the upper Tortonian sediments in the foreland basins, significant counterclockwise rotations have been evidenced in the thrust top Taouinate-Tefrant-Dhar Souk basins, located in the Rif orogenic wedge. These paleomagnetic results indicate that counterclockwise rotations, previously measured in the Mesozoic units of the Rif chain, extended also into upper Miocene units of the chain. This makes substantially younger the age of counterclockwise rotation in the Rif chain and suggests that the bending of the Gibraltar Arc could not completely be achieved in the late Miocene. Our results imply a reconsideration of the timing of paleomagnetic rotations in the Rif and, together with those obtained by Mattei et al. [2006] enhance the role of vertical axis rotations in the late Miocene to Recent tectonic evolution of the Gibraltar Arc.

[37] **Acknowledgments.** The authors would like to thank Associate Editor Stuart Gilder, an anonymous reviewer, and Dominique Frizon de Lamotte for the constructive reviews of the manuscript. We would also like to thank F. Rossetti, C. Faccenna, and D. El Azzab for participating to the paleomagnetic sampling. Financial support for this work was provided by 01-LECEMA22F (WESTMED); by the European Science Foundation under the EUROCORES Programme EUROMARGINS, through contract ERAS-CT-2003-980409 of the European Commission, DG Research, FP6; and by COFIN-2004 MIUR research program.

References

- Ait Brahim, L., and B. A. Chotin (1989), Genèse et déformation des bassins néogènes du Rif central (Maroc) au cours du rapprochement Europe-Afrique, *Geodin. Acta*, 3, 295–304.

- Akoglu, A., Z. Cakir, M. Meghraoui, S. Belabbes, S. O. El Alami, S. Ergintav, and H. S. Akyuz (2006), The 1994–2004 Al Hoceima (Morocco) earthquake sequence: Conjugate fault ruptures deduced from InSAR, *Earth Planet. Sci. Lett.*, 252, 467–480.
- Balanyá, J. C., V. García-Dueñas, J. M. Azañón, and M. Sánchez-Gómez (1997), Alternating contractional and extensional events in the Alpujarra nappes of the Alboran Domain (Betics, Gibraltar Arc), *Tectonics*, 16, 226–238.
- Ben Yaich, A., G. Duec, P. Souquet, and M. J. Fondécave-Wallez (1989), Les grès de Zoumi: Dépôt turbiditique d'une avant-fosse miocène (Burdigalien-Serravalien) dans le Rif occidental (Maroc), *C. R. Acad. Sci., Ser. II*, 309, 1819–1825.
- Bermini, M., M. Boccaletti, G. Moratti, and G. Papani (2000), Structural development of the Taza-Guercif Basin as a constraint for the Middle Atlas Shear Zone tectonic evolution, *Mar. Pet. Geol.*, 17, 391–408.
- Besse, J., and V. Courtillot (2002), Apparent and true polar wander and the geometry of the geomagnetic field over the last 200 Myr, *J. Geophys. Res.*, 107(B11), 2300, doi:10.1029/2000JB000050.
- Biggs, J., E. Bergman, B. Emmerson, G. J. Funning, J. Jackson, B. Parsons, and T. J. Wright (2006), Fault identification for buried strike-slip earthquakes using InSAR: The 1994 and 2004 Al Hoceima, Morocco earthquakes, *Geophys. J. Int.*, 166, 1347–1362.
- Blanco, M. J., and W. Spakman (1993), The P-wave velocity structure of the mantle below the Iberian Peninsula: Evidence for subducted lithosphere below southern Spain, *Tectonophysics*, 221, 13–34.
- Butler, R. F. (1992), *Paleomagnetism: Magnetic Domains to Geologic Terranes*, 319 pp., Blackwell, Oxford, U.K.
- Calvert, A., E. Sandvol, D. Seber, M. Barazangi, F. Vidal, G. Alguacil, and N. Jabour (2000), Propagation of regional seismic phases (Lg and Sn) and Pn velocity structure along the Africa-Iberia plate boundary zone: Tectonic implications, *Geophys. J. Int.*, 142, 384–408.
- Chalouan, A., A. Michard, H. Feinberg, R. Montigny, and O. Saddiqi (2001), The Rif mountain building (Morocco): A new tectonic scenario, *Bull. Soc. Geol. Fr.*, 172, 603–616.
- Cifelli, F., M. Mattei, and F. Rossetti (2007), Tectonic evolution of arcuate mountain belts on top of a retreating subduction slab: The example of the Calabrian Arc, *J. Geophys. Res.*, 112, B09101, doi:10.1029/2006JB004848.
- Comas, M. C., J. P. Platt, J. I. Soto, and A. B. Watts (1999), The origin and tectonic history of the Alboran Basin: Insights from Leg 161 results, *Proc. Ocean Drill. Program Sci. Results*, 161, 555–580.
- Crespo-Blanc, A., and D. Frizon de Lamotte (2006), Structural evolution of the external zones derived from the Flysch Through and the South Iberian and Maghrebian paleomargins around the Gibraltar Arc: A comparative study, *Bull. Soc. Geol. Fr.*, 177, 267–282.
- Demarest, H. H. (1983), Error analysis for the determination of tectonic rotation from paleomagnetic data, *J. Geophys. Res.*, 88, 4321–4328.
- Duggen, S., K. Hoernle, P. van den Bogaard, L. Rüpke, and J. P. Morgan (2003), Deep roots of the Messinian salinity crisis, *Nature*, 422, 602–606.
- Durand-Delga, M., L. Hottinger, J. Marçais, M. Mattauer, Y. Milliard, and G. Suter (1962), Données actuelles sur la structure du Rif, in *Livre à la Mémoire de Professeur Fallot*, edited by M. Durand-Delga, *Mem. Soc. Geol. Fr.*, 1, 241–247.
- Durand-Delga, M., P. Rossi, P. H. Olivier, and D. Puglisi (2000), Situation structurale et nature ophiolitique de roches basiques jurassiques associées aux flyschs maghrébins du Rif (Maroc) et de Sicile (Italie), *C. R. Acad. Sci.*, 331, 29–38.
- Faccenna, C., C. Pirrallo, A. Crespo-Blanc, L. Jolivet, and F. Rossetti (2004), Lateral slab deformation and the origin of the western Mediterranean arcs, *Tectonics*, 23, TC1012, doi:10.1029/2002TC001488.
- Fadil, A., P. Vernant, S. McClusky, R. Reilinger, F. Gomez, D. Ben Sari, T. Mourabit, K. Feigl, and M. Barazangi (2006), Active tectonics of the western Mediterranean: Geodetic evidence for rollback of a delaminated subcontinental lithospheric slab beneath the Rif Mountains, Morocco, *Geology*, 34(7), 529–532.
- Favre, P. (1995), Analyse quantitative du rifting et de la relaxation thermique de la partie occidentale de la marge transformante nord-africaine: Le Rif externe (Maroc). Comparaison avec la structure actuelle de la chaîne, *Geodin. Acta*, 8, 59–81.
- Fisher, R. A. (1953), Dispersion on a sphere, *Proc. R. Soc. London, Ser. A*, 217, 295–305.
- Flinch, J. F. (1996), Accretion and extensional collapse of the external Western Rif (Northern Morocco), in *Structure and Prospects of Alpine Basins and Forelands*, edited by P. A. Ziegler and F. Horvath, *Mem. Mus. National Hist. Nat.*, 170, 61–85.
- Frizon de Lamotte, D., J. Andrieux, and J. C. Guézou (1991), Cinématique des chevauchements néogènes dans l'Arc bético-rifain: Discussion sur les modèles géodynamiques, *Bull. Soc. Geol. Fr.*, 162, 611–626.
- Frizon de Lamotte, D., et al. (2004), TRANSMED-transect I [Betics, Alboran Sea, Rif, Moroccan Meseta, High Atlas, Jbel Saghro, Tindouf basin], in *The TRANSMED Atlas—The Mediterranean Region From Crust to Mantle*, edited by W. Cavazza et al., 141 pp. + CD-ROM, Springer, Berlin.
- García-Dueñas, V., J. C. Balanyá, and J. M. Martínez-Martínez (1992), Miocene extensional detachments in the outcropping basement of the northern Alboran basin (Betics) and their tectonic implications, *Geo Mar. Lett.*, 12, 88–95.
- Guillemin, M., and J. P. Houzay (1982), Le néogène post-nappes et le Quaternaire du Rif nord-oriental: Stratigraphie et tectonique des bassins de Melilla, du Kert, de Boudinar et du piémont des Keddana, *Notes Mem. Serv. Geol. Maroc*, 314, 1–238.
- Gutscher, M. A. (2004), What caused the great Lisbon earthquake?, *Science*, 305, 1247–1248.
- Gutscher, M. A., J. Malod, J.-P. Rehault, I. Contrucci, F. Klingelhoefer, L. Mendes-Victor, and W. Spakman (2002), Evidence for active subduction beneath Gibraltar, *Geology*, 30, 1071–1074.
- Hilgen, F. J., L. Bissoli, S. Iaccarino, W. Krijgsman, R. Meijer, A. Negri, and G. Villa (2000), Integrated stratigraphy and astrochronology of the Messinian GSSP at Oued Akrech (Atlantic Morocco), *Earth Planet. Sci. Lett.*, 182, 237–251.
- Jolivet, L., and C. Faccenna (2000), Mediterranean extension and the Africa-Eurasia collision, *Tectonics*, 19(6), 1095–1106.
- Kissel, C., and C. Laj (1988), The Tertiary geodynamical evolution of the Aegean arc: A paleomagnetic reconstruction, *Tectonophysics*, 146, 183–201.
- Kirschvink, J. L. (1980), The least-squares line and plane and the analysis of paleomagnetic data, *Geophys. J. R. Astron. Soc.*, 62, 699–718.
- Krijgsman, W., and M. Garcés (2004), Pleomagnetic constrains on the geodynamic evolution of the Gibraltar Arc, *Terra Nova*, 16, 281–287.
- Krijgsman, W., C. G. Langereis, W. J. Zachariasse, M. Boccaletti, G. Moratti, R. Gelati, S. Iaccarino, G. Papani, and G. Villa (1999), Late Neogene evolution of the Taza-Guercif Basin (Rifian Corridor, Morocco) and implications for the Messinian salinity crisis, *Mar. Geol.*, 153, 147–160.
- Krijgsman, W., S. Gaboardi, F. J. Hilgen, S. Iaccarino, E. de Kaenel, and E. Van der Laan (2004), Revised astrochronology for the Ain el Beida section (Atlantic Morocco): No glacio-eustatic control for the onset of the Messinian Salinity Crisis, *Stratigraphy*, 1, 87–101.
- Leblanc, D., and P. Olivier (1984), Role of strike-slip faults in the Betic Rifian Orogeny, *Tectonophysics*, 101, 344–355.
- Loneragan, L., and N. White (1997), Origin of the Betic-Rif mountain belt, *Tectonics*, 16(3), 504–522.
- Lowrie, W. (1990), Identification of ferromagnetic minerals in a rock by coercivity and unblocking temperature properties, *Geophys. Res. Lett.*, 17, 159–162.
- Mattei, M., F. Cifelli, I. M. Rojas, A. Crespo-Blanc, M. C. Comas, C. Faccenna, and M. Porreca (2006), Neogene tectonic evolution of the Gibraltar Arc: New paleomagnetic constrains from the Betic chain, *Earth Planet. Sci. Lett.*, 250, 522–540.
- Mattei, M., F. Cifelli, and N. D'Agostino (2007), The evolution of the Calabrian Arc: Evidence from paleomagnetic and GPS observations next term, *Earth Planet. Sci. Lett.*, 263(3–4), 259–274, doi:10.1016/j.epsl.2007.08.034.
- Mc Clusky, S., R. Reilinger, S. Mahmoud, D. Ben Sari, and A. Tealeb (2003), GPS constraints on Africa (Nubia) and Arabia plate motions, *Geophys. J. Int.*, 155, 126–138.
- McFadden, P. L. (1990), A new fold test for paleomagnetic studies, *Geophys. J. Int.*, 103, 163–169.
- McFadden, P. L., and M. W. McElhinny (1988), The combined analysis of remagnetization circles and direct observations in paleomagnetism, *Earth Planet. Sci. Lett.*, 87, 161–172.
- McFadden, P. L., and M. W. McElhinny (1990), Classification of the reversal test in palaeomagnetism, *Geophys. J. Int.*, 103, 725–729.
- Meghraoui, M., J. L. Morel, J. Andrieux, and M. Dahmani (1996), Tectonique plioquaternaire de la chaîne tello-rifaine et de la mer d'Alboran: Une zone complexe de convergence continent-continent, *Bull. Soc. Geol. Fr.*, 167, 141–157.
- Michard, A., D. Frizon de Lamotte, and A. Chalouan (2005), Comment on “The ultimate arc: Differential displacements, oroclinal bending, and vertical axis rotation in the External Betic-Rif arc” by J. P. Platt et al., *Tectonics*, 24, TC1005, doi:10.1029/2003TC001603.
- Morales, J., I. Serrano, A. Jabaloy, J. Galindo-Zaldivar, D. Zhao, F. Torcal, F. Vidal, and F. Gonzalez-Lodeiro (1999), Active continental subduction beneath the Betic Cordillera and the Alboran Sea, *Geology*, 27, 753–758.
- Morley, C. K. (1988), The tectonic evolution of the Zoumi Sandstone, western Moroccan Rif, *J. Geol. Soc. London*, 145, 55–63.
- Morley, C. K. (1992), Tectonic and sedimentary evidence for synchronous and out-of-sequence thrusting Larache-Acilah area, western Morocco Rif, *J. Geol. Soc. London*, 149, 39–49.
- Platt, J., and R. L. M. Vissers (1989), Extensional collapse of thickened continental lithosphere: A working hypothesis for the Alboran Sea and Gibraltar Arc, *Geology*, 17, 540–543.

- Platt, J. P., S. Allerton, A. Kirker, C. Mandeville, A. Mayfield, E. S. Platzman, and A. Rimi (2003), The ultimate arc: Differential displacement, oroclinal bending, and vertical axis rotation in the External Betic-Rif arc, *Tectonics*, 22(3), 1017, doi:10.1029/2001TC001321.
- Platzman, E. S. (1992), Paleomagnetic rotations and the kinematics of the Gibraltar Arc, *Geology*, 20, 311–314.
- Platzman, E. S., J. P. Platt, and P. Olivier (1993), Palaeomagnetic rotations and fault kinematics in the Rif arc of Morocco, *J. Geol. Soc. London*, 150, 707–718.
- Royden, L. (1993), The tectonic expression of slab pull at convergent plate boundaries, *Tectonics*, 12, 303–325.
- Samaka, F., A. Benyaich, M. Dakki, M. Hcaine, and A. W. Bally (1997), Origine et inversion des bassins miocènes supra-nappes du Rif Central (Maroc), Etude de surface et de subsurface, *Geodin. Acta*, 10, 30–40.
- Sani, F., M. Zizi, and A. W. Bally (2000), The Neogene-Quaternary evolution of the Guercif Basin (Morocco) reconstructed from seismic line interpretation, *Mar. Pet. Geol.*, 17, 343–357.
- Scheepers, P. J. J. (1992), No tectonic rotation for the Apulia-Gargano foreland in the Pleistocene, *Geophys. Res. Lett.*, 19(22), 2275–2278.
- Seber, D., M. Barazangi, A. Ibenbrahim, and A. Demnati (1996), Geophysical evidence for lithospheric delamination beneath the Alboran Sea and Rif-Betic mountains, *Nature*, 379, 785–790.
- Speranza, F., L. Sagnotti, and M. Mattei (1997), Tectonics of the Umbria-Marche-Romagna arc (central northern Apennines, Italy): New paleomagnetic constrains, *J. Geophys. Res.*, 102, 3153–3166.
- Speranza, F., R. Maniscalco, M. Mattei, A. Di Stefano, R. W. H. Butler, and R. Funicello (1999), Timing and magnitude of rotations in the frontal thrust systems of southwestern Sicily, *Tectonics*, 18, 1178–1197.
- Stich, D., E. Serpelloni, F. de Lis Mancilla, and J. Morales (2006), Kinematics of the Iberia-Maghreb plate contact from seismic moment tensors and GPS observations, *Tectonophysics*, 426, 295–317.
- Suter, G. (1980), Carte géologique de la Chaîne Rifaine, scale 1:500,000, Serv. Géol. du Maroc, Rabat.
- Tejera de Leon, J., M. Boutakiout, A. Ammar, L. Ait Brahim, and N. El Hatimi (1995), Les bassins du Rif central (Maroc): Marqueurs de chevauchements hors séquence d'âge miocène terminal au cœur de la chaîne, *Bull. Soc. Geol. Fr.*, 166, 751–761.
- Tejera de Leon, J., A. Ammar, M. Boutakiout, L. Ait Brahim, and N. El Hatimi (1996), Le Bassin néogène de Tounate: Un bassin synorogénique de propagation de rampe (Rif central-Maroc), *Notes Mem. Serv. Geol. Maroc*, 387, 21–32.
- Van Assen, E., K. F. Kuiper, W. Krijgsman, F. J. Sierro, and N. Barhoun (2004), Messinian astrochronology of the Melilla basin: Stepwise restriction of the Mediterranean-Atlantic connection through Morocco, *Palaeogeogr. Palaeoclimatol. Palaeoecol.*, 238(1–4), 15–31.
- Wernli, R. (1988), Micropaléontologie du Néogène post-nappes du Maroc septentrional et description systématique des foraminifères planctoniques, *Notes Mem. Serv. Geol. Maroc*, 331, 266 pp.
- Wildi, W. (1983), La chaîne tello-rifaine (Algérie, Maroc, Tunisie): Structure, stratigraphie et évolution du trias au Miocène, *Rev. Geol. Dyn. Geogr. Phys.*, 24, 201–297.
- Zeck, H. P. (1999), Alpine plate kinematics in the western Mediterranean: A westward directed subduction regime followed by slab rollback and slab detachment, in *The Mediterranean Basins: Tertiary Extension Within the Alpine Orogen*, edited by B. Durand et al., *Geol. Soc. Spec. Publ.*, 156, 109–120.

F. Cifelli, M. Mattei, and M. Porreca, Dipartimento di Scienze Geologiche, Università Roma Tre, Largo San Leonardo Murialdo 1, Roma, I-00146, Italy. (cifelli@uniroma3.it)